ChemComm

COMMUNICATION

View Article Online
View Journal | View Issue

Cite this: *Chem. Commun.*, 2015, **51**, 17732

Received 7th August 2015,
Accepted 15th October 2015

DOI: 10.1039/c5cc06642e

www.rsc.org/chemcomm

Record high magnetic exchange and magnetization blockade in $Ln_2@C_{79}N$ (Ln = Gd(III) and Dy(III)) molecules: a theoretical perspective†

Mukesh Kumar Singh, Neeraj Yadav and Gopalan Rajaraman*

***Ab initio* and DFT calculations reveal a very strong ferromagnetic exchange of the order of 200 cm^{-1} in an endohedral radical hetero-metallo-fullerene molecule $Gd_2@C_{79}N$. Calculations performed on the anisotropic $Dy_2@C_{79}N$ molecule reveal that very strong Dy–radical exchange not only quenches the QTM effects but also immensely enhances the barrier height for magnetization reversal.**

Single molecule magnets are an attractive area of research due to numerous potential applications proposed for this class of molecules.[1] There are several hurdles in realising these applications, particularly controlling the spin Hamiltonian parameters such as the spin ground state, magnetic anisotropy, intra- and intermolecular interactions are the top challenges to address in this area.[2] As controlling the zero-field splitting parameter in transition metal clusters is challenging, research groups have moved to lanthanide based SMMs as they inherit very large anisotropy.[3] Large anisotropy due to very large spin–orbit coupling leads to an extremely large barrier height for magnetization reversal and to date several molecules have been reported to possess barrier heights greater than the desired 300 K.[4] However large spin–orbit coupling under low symmetry conditions also aids in the mixing of wave functions, leading to the undesired faster quantum tunnelling of magnetization (QTM) between the ground/excited states. This drastically reduces the blocking temperature of this class of molecules.[5] There are two approaches proposed to quench the QTM effects: (i) preserving a very high-symmetry around the lanthanide ion reduces the mixing of states and (ii) inducing splitting of m_J levels *via* exchange coupling with other lanthanide/transition metal/radical ions also serves the purpose.[5c,6] Elegant examples for both categories are available; $[TbPc_2]$ and $\{Dy_4K_2\}$ molecules possess high symmetry around the lanthanide ions and thus reduce tunnelling while inducing coupling with metal ions/radicals leading to the isolation of $\{Dy_2Cr_2\}$ and $\{TbN_2^{3-}\}$ complexes possessing very high blocking temperatures.[5d,6b,c,7] Despite these breakthrough achievements, a rational approach to achieve very large magnetic coupling as required to reach large T_B is not available. These parameters are often difficult to control in classical coordination complexes.[8]

In this regard, metal encapsulated fullerenes, *i.e.* endohedral metallo-fullerenes (EMFs), in which the metal ions are encapsulated inside the cage molecule, are ideal candidates in which symmetry, exchange interaction and dipolar interaction can be controlled easily.[9] Several lanthanide encapsulated EMFs have been reported in the literature and some of them have also been found to exhibit SMM characteristics.[10] Among the EMFs, the most promising class of molecules are radical based fullerenes as these offer direct-exchange between the encapsulated lanthanide ions and the radical cage. In this regard, the report of $(C_{79}N)^{6-}$ hetero-fullerene radicals has gained importance as they have been characterized thoroughly and the crystal structure encapsulating different lanthanide ions has been reported.[11] Of particular importance is the Gd(III) analogue $Gd_2@C_{79}N$, in which the ground state is estimated to be $S = 15/2$ arising from strong Gd(III)–radical exchange as revealed by several techniques including HF-EPR study.[12]

In this work, we aim to compute the magnetic exchange coupling present in the $Gd_2@C_{79}N$ molecule and extend the work to the anisotropic $Dy_2@C_{79}N$ cage using DFT and the CASSCF + RASSI-SO/POLY_ANISO approach using the MOLCAS code.[13] The mechanism of magnetic relaxation and how the radical–Dy(III) interaction quench the QTM effects are explored. The B3LYP/TZV (CSDZ for Gd(III)) combination has a proven track record to yield accurate structures and properties for this class of molecules.[14] To test the methodology further, we have studied the radical C_{82}^{3-} cage with Gd(III), *i.e.* the $Gd@C_{82}$ molecule and the computed structures and magnetic coupling constants are in agreement with experiments.[15] This offers confidence in the employed methodology (see ESI,† for details). For the $Gd_2@C_{79}N$ molecule, based on the position of the N atom there are two possible isomers, $Gd_2@666\text{-}(C_{79}N)$ and $Gd_2@665\text{-}(C_{79}N)$ (see Fig. 1a).[12] The former one has the N atom at the junction of three hexagonal sites while the latter one has the nitrogen atom at a junction of two hexagonal and one pentagonal sites (see Fig. 1a and

Department of Chemistry, Indian Institute of Technology Bombay, Powai, Mumbai, Maharashtra, 400076-India. E-mail: rajaraman@chem.iitb.ac.in; Tel: +91-22-2576-7187

† Electronic supplementary information (ESI) available: Optimized structures, CASSCF + RASSI-SO energies, spin density plots, overlap integrals, and the NBO data mechanism of relaxation along with computational details. See DOI: 10.1039/c5cc06642e

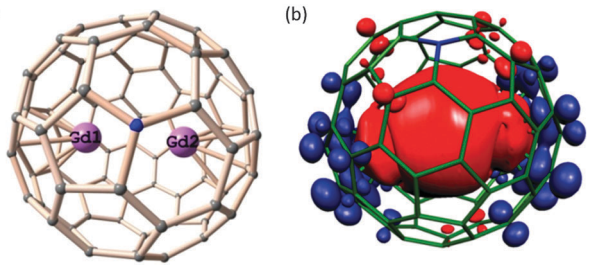

Fig. 1 (a) DFT optimized structure of the Gd_2@665-($C_{79}N$) isomer along with (b) its spin density plot for the S = 15/2 state.

Fig. S1 of ESI†).[10a,16] The computed Gd–C bond lengths are found to be in the range of 2.410–2.673 Å for the Gd_2@665-($C_{79}N$) isomer whereas for the Gd_2@666-($C_{79}N$) isomer, they are found in the range of 2.403–2.738 Å. Here the Gd_2@665-($C_{79}N$) isomer is found to be stabilized by 61.6 kJ mol^{-1} compared to the Gd_2@666-($C_{79}N$) isomer (energy difference is merely 17.3 kJ mol^{-1} for the bare $C_{79}N$ cage; see Table S1 of ESI,† for selected structural parameters and the computed energies).

As the two Gd(III) centres are symmetric, there are two exchange interactions present in this cluster: J_1 interaction describes coupling between the $C_{79}N$ radical and the Gd(III) ions while J_2 interaction describes the coupling between two Gd(III) ions. The J_1 and J_2 interactions are estimated to be +200 cm^{-1} and −0.4 cm^{-1} respectively, for the lowest lying Gd_2@665-($C_{79}N$) isomer. For the Gd_2@666-($C_{79}N$) isomer on the other hand, calculations yield a similar set of J constants (J_1 = +189 cm^{-1} and J_2 = −0.4 cm^{-1} using $\hat{H} = -2JS_{Gd}S_{rad}$ Hamiltonian Fig. S2 of ESI†). Quite interestingly, the Gd(III)–radical exchange estimated here is the largest exchange interaction known. The second largest J value reported for this type of interaction is in the $\{Gd_2N_2^{3-}\}$ complex where the radical–Gd(III) J is estimated to be −27 cm^{-1}.[5c,17] The J values reported for all the other radical–Gd(III) complexes are an order of magnitude less compared to this estimate.[8] Although the exact value of J has not been uniquely determined, the experimental data suggest strong ferromagnetic exchange between the Gd(III) and the radical leading to the 15 line EPR signal corresponding to the S = 15/2 ground state. The signals are visible even at higher temperatures suggesting the isolated ground state at these temperatures. Besides, pulsed EPR measurements reveal a very long spin relaxation leading to the detection of an electron spin echo signal even at 20 K. This also indicates strong Gd(III)–radical interaction.[18] Although the radical–Gd(III) interaction is very strong, the Gd(III)–Gd(III) interaction is estimated to be weak and antiferromagnetic in nature. This is in accordance with the long metal–metal distance (3.8 Å) offering small exchange interaction. To understand the origin of the strong exchange interaction, we have analysed the molecular orbitals, NBOs and spin densities (see Fig. 1b for spin density plot of S = 15/2 state; see Fig. S3 and S4 in ESI,† for plots of other spin states). We have earlier established the mechanism (see Fig. S5 of ESI†) of magnetic coupling in Gd(III)–radical and {3d-Gd} complexes[8,14,19] where the ferromagnetic contribution to the J values is found to arise due to orbital orthogonality between the SOMOs (see Fig. S6, ESI,† for computed overlap integrals) and the charge-transfer contribution from the radical centre to the empty 5d/6s/6p orbitals of the Gd(III) (see Fig. S7 and Table S2 of ESI†). The sole antiferromagnetic contribution to J arises from the overlap of the π* orbital of the radical with the 4f orbitals of the Gd(III) which is found to be weak here. Here there is direct exchange between Gd(III) and the $C_{79}N$ radical molecule. As the HOMO of $C_{79}N^{6-}$ is low-lying in energy, there is a substantial charge-transfer from the $C_{79}N$ unit to both the Gd(III) atoms, leading to a significant gain in the spin density at the Gd(III) centres. The NBO analysis in fact reveals a $4f^7 5d^{0.6}$ electronic configuration revealing the extent of charge-transfer to the Gd(III) empty orbitals. The spin densities on the Gd(III) centres are also found to be higher than the expected value (∼7.45 on each Gd(III) centres). This leads to a very strong coupling between the radical and the Gd(III) centre. The spin density plot also reveals a significant polarization on the $C_{79}N$ unit. As the spin density on the hetero-fullerene $C_{79}N$ is localized on the nitrogen atom, this facilitates efficient charge transfer while such behaviour was not observed in the homo-fullerene such as C_{82}^{3-}. The charge-transfer is also clearly visible in the NBO second order donor–acceptor interactions (see Fig. S8 in ESI†). The EPR study undertaken earlier on the Y_2@$C_{79}N$ complex yields anisotropic g-tensors, and hyperfine tensors of Y(III) atoms are visible.[11b] This indicates that the unpaired electrons are certainly not localized on the $C_{79}N$ cage but are largely delocalized also on the Y(III) atoms. This supports our charge-transfer proposal to the Gd(III) centres in the Gd_2@$C_{79}N$ cage. Besides, our additional calculations performed on La_2@$C_{79}N$ clearly reveal that delocalisation takes place only when there is a radical centre (see Table S3 of ESI†).

Since the magnetic coupling is estimated to be very large, we have modelled the Dy_2@665-($C_{79}N$) molecule to explore the possibility of obtaining high blocking temperatures and quenching of QTM effects. We have performed *ab initio* CASSCF + RASSI-SO/SINGLE_ANISO/POLY_ANISO calculations using the MOLCAS 7.8 code (see ESI,† for computational details†). Analysis of both the single-ion anisotropy and the exchange anisotropy has been performed to predict the magnetisation relaxation process. The Dy1 (Dy2) ions are found to coordinate in an $\eta_7(\eta_6)$ fashion with the hexagonal ring, offering strong interaction (Dy–C distances are estimated to be 2.4 to 2.6 Å) in one of the axial directions. In the other axial direction, only a weak interaction due to the second Dy(III) ion is present. This along with a negligible equatorial interaction for both the Dy(III) centres ideally suits the oblate Dy(III) ion. The coordination environment could perhaps be compared to the mono-coordinated Dy(III)–O model studied earlier by Chibotaru and co-workers.[20] We have computed eight-low lying Kramer's Doublets (KDs) for both Dy(III) ions separately, corresponding to the $^6H_{15/2}$ state. These states are found to lie within an energy span of 837.6 cm^{-1} and 785.7 cm^{-1} for Dy1 and Dy2 sites, respectively, with $m_J = \pm 15/2$ stabilized as the ground state. The computed ground state anisotropy for both Dy(III) ions are found to be purely Ising in nature (Dy1, g_{xx} = 0.001, g_{yy} = 0.002, g_{zz} = 19.979 and Dy2, g_{xx} = 0.001, g_{yy} = 0.002 and g_{zz} = 19.881,) suggesting very small QTM effects within the ground state KD (QTM = 0.0006 μ_B for both Dy1 and Dy2 ions; see Fig. S9 and Table S4 of ESI†). The ground state g_{zz} axes for both the Dy(III) ions are found to be oriented along the pseudo C_6 axis present in the hexagonal ring (see Fig. 2a). The first excited state KDs lie at 245 cm^{-1} and 134 cm^{-1} higher in energy for Dy1 and Dy2 ions, respectively. These first excited KDs for Dy1 and Dy2 ions are

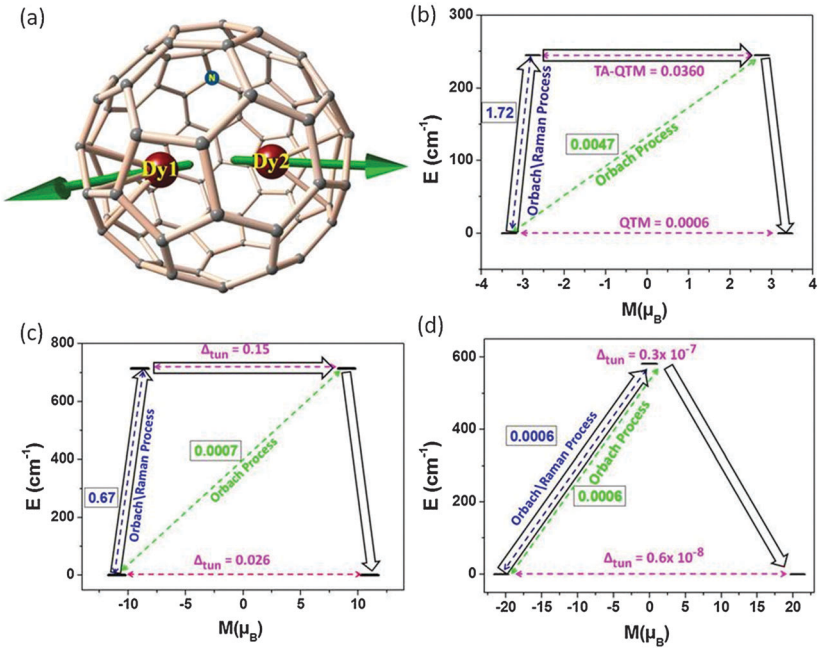

Fig. 2 (a) Ground state KD orientation for both Dy(III) ions of Dy_2@665-($C_{79}N$); (b) *ab initio* SINGLE_ANISO computed magnetization blockade barrier for the Dy1 ion; (c) *ab initio* POLY_ANISO computed magnetization blockade barrier for Dy1–radical exchange coupled systems for the DyLu@665-($C_{79}N$) model and (d) *ab initio* POLY_ANISO computed magnetization blockade barrier for Dy1–Dy2@665-($C_{79}N$). In (b–d) the *x*-axis indicates the magnetic moment of each state along the main magnetic axis while the *y*-axis denotes the energy of the respective states. The thick black lines imply Kramer's doublet as a function of magnetic moment. The dotted green and blue lines indicate the possible pathway of the Orbach/Raman contribution of magnetic relaxation. The hollow black arrows indicate the most probable relaxation pathway for the magnetization reorientation. The dotted red lines correspond to the QTM/TA-QTM/$\Delta_{tunneling}$ relaxation contributions between the connecting pairs. The numbers provided at each arrow are the mean value for the corresponding matrix element of the magnetic moment.

also found to be Ising in nature with small transverse components (Dy1, g_{xx} = 0.083, g_{yy} = 0.120, g_{zz} = 17.119 and Dy2, g_{xx} = 0.011, g_{yy} = 0.014 and g_{zz} = 17.453). The computed transversal magnetic moments between the first excited KDs are found to be smaller in both Dy(III) ions (0.0360 μ_B and 0.0047 μ_B for Dy1 and Dy2 respectively), suggesting very small TA-QTM to be operative through the first excited KD. The Orbach/Raman process related to the ground state and the first excited state of opposite magnetization is also found to be very small (0.0047 μ_B and 0.0022 μ_B for Dy1 and Dy2 respectively) but relaxation within the same sign states (+1 to +2) is found to be large (1.7 μ_B for both Dy(III) ions). With respect to the ground state g_{zz} axis, the first excited g_{zz} axis is found to be tilted by 7.7° and 16.1° for Dy1 and Dy2 respectively (see Fig. S9 and Table S4 of ESI†). Due to this deviation, relaxation is expected to occur *via* the first excited state and this results in the U_{cal} values of 244.5 cm^{-1} and 134.3 cm^{-1} for Dy1 and Dy2 ions, respectively. As the coordination mode between Dy1 and Dy2 sites is different, with Dy1 interacting strongly with the $C_{79}N$ compared to the Dy2 ion, this difference is rather expected. Besides this analysis, the computed crystal field parameter B_q^k also offers insights into the relaxation mechanism. Smaller non-axial B_q^k (where $q \neq 0$, k = 2, 4, 6) terms compared to their corresponding axial B_q^k (where q = 0, k = 2, 4, 6) terms are found to obstruct the QTM process. The ground state KD of both Dy(III) ions possesses a larger axial crystal field parameter while the first excited state is found to possess both the axial and the non-axial terms leading to relaxation *via* the first excited state KD (see Tables S5 and S6 of ESI†).

To understand the mechanism of magnetic relaxation of the full molecule, we have modelled two structures; in the first model we have considered only one Dy(III) ion by replacing the other with the Lu(III) ion (DyLu/LuDy@$C_{79}N$ models). The Dy(III)–radical exchange is estimated to be +285.7 cm^{-1} (see ESI,† for details), with this exchange coupling, we have simulated the exchange coupled states using the POLY_ANISO program considering an isotropic ***g***-tensor for the radical centre. The ground state is estimated to be a pure Ising type with the g_{zz} value of 21.981 (g_{xx} and g_{yy} are virtually zero) and the first excited state is estimated to lie at 713 cm^{-1} higher in energy. Besides, the tunnel splitting (Δ_{tun}) of the ground state is also computed to be small (2.6×10^{-2} cm^{-1}) and relaxation is expected to occur *via* the first excited state possessing larger Δ_{tun}. This results in the U_{cal} value of 713 cm^{-1} for the DyLu@$C_{79}N$ model which is *ca.* three times higher than what is computed for the mononuclear Dy(III) ions without the radical counterpart. This U_{cal} estimated here is one of the largest estimated and more importantly the strong exchange likely to quench the QTM significantly offers also very high blocking temperatures.[1d,6a,7b,c] For the second Dy2–radical combination, the same is estimated to be 711 cm^{-1} (see Table S7 of ESI†). In the second step, we have considered both the Dy(III) ions together in combination with the radical. Employing Dy–radical exchange of +285.7 cm^{-1} (using $\hat{H} = -JS_{Dy}S_{rad}$) along with a weak Dy(III)–Dy(III) exchange of −0.3 cm^{-1} leads to the blockade barrier as shown in Fig. 2d. The ground state is estimated to be pure Ising type and the Δ_{tun} is estimated to be very small. The stronger Dy–radical exchange and weaker Dy(III)–Dy(III) exchange

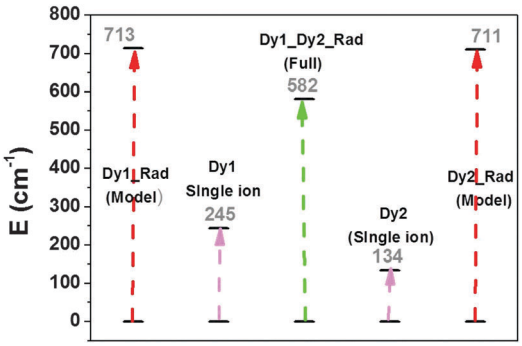

Fig. 3 Diagrammatic comparison of barrier heights (U_{cal} values) estimated for different models studied for the Dy_2@665-$C_{79}N$ molecule.

place the first excited state at 582.2 cm^{-1} which is again higher than that computed for single-ion Dy(III) centres (see Fig. 3). Although the Δ_{tun} of the first excited state is also small, the first excited state g_{zz} axis is tilted by 91.0° compared to the ground state KD (see Fig. S10 of ESI†). This suggests relaxation to occur *via* the first excited state leading to an U_{cal} value of 582.2 cm^{-1}. Although the value is among the largest reported, the higher value is essentially due to exchange interaction, which additionally quenches the QTM. Other relaxation pathways such as intermolecular interactions are also expected to be minimal here as the metal ion is encapsulated inside the cage increasing the chance of observing a large T_B for this molecule. Although anisotropic Ln_2@$C_{79}N$ molecules are synthesized, magnetic studies in this direction have not been pursued yet.[11b]

To this end, our theoretical search for a very strong magnetic exchange in lanthanide–radical systems lead us to endohedral metallo hetero-fullerene molecules in which extremely large magnetic exchange interactions are detected. Direct exchange and significant charge transfer offered by the radical hetero-fullerenes lead to very large J values that cannot possibly be achieved in classical lanthanide coordination complexes. Besides, the Dy_2@665-($C_{79}N$) molecule studied here was found to yield a larger barrier height compared to the corresponding single-ion Dy(III) anisotropy. This observation is the first of its kind where the magnetic exchange was not only found to quench the QTM effects but was also found to help enhance the barrier height significantly. Our predictions warrant magnetic studies on these molecules and theoretical studies on other EMFs possessing interesting magnetic properties are underway in our laboratory.

GR would like to acknowledge DST (EMR/2014/000247), INSA and DST Nanomission for funding and MKS thanks UGC for a fellowship.

References

1 (*a*) M. N. Leuenberger and D. Loss, *Nature*, 2001, **410**, 789; (*b*) L. Bogani and W. Wernsdorfer, *Nat. Mater.*, 2008, **7**, 179; (*c*) G. Christou, D. Gatteschi, D. N. Hendrickson and R. Sessoli, *MRS Bull.*, 2000, **25**, 66; (*d*) R. Sessoli, D. Gatteschi, A. Caneschi and M. A. Novak, *Nature*, 1993, **365**, 141; (*e*) F. Neese and D. A. Pantazis, *Faraday Discuss.*, 2011, **148**, 229.
2 E. Ruiz, J. Cirera, J. Cano, S. Alvarez, C. Loose and J. Kortus, *Chem. Commun.*, 2008, 52.
3 (*a*) C. Benelli, A. Caneschi, D. Gatteschi and R. Sessoli, *Adv. Mater.*, 1992, **4**, 504; (*b*) S. Osa, T. Kido, N. Matsumoto, N. Re, A. Pochaba and J. Mrozinski, *J. Am. Chem. Soc.*, 2004, **126**, 420; (*c*) J. D. Leng, J. L. Liu, W. Q. Lin, S. Gomez-Coca, D. Aravena, E. Ruiz and M. L. Tong, *Chem. Commun.*, 2013, **49**, 9341; (*d*) L. Sorace, C. Benelli and D. Gatteschi, *Chem. Soc. Rev.*, 2011, **40**, 3092.
4 S. D. Jiang, B. W. Wang, H. L. Sun, Z. M. Wang and S. Gao, *J. Am. Chem. Soc.*, 2011, **133**, 4730.
5 (*a*) D. Tanaka, T. Inose, H. Tanaka, S. Lee, N. Ishikawa and T. Ogawa, *Chem. Commun.*, 2012, **48**, 7796; (*b*) A. Watanabe, A. Yamashita, M. Nakano, T. Yamamura and T. Kajiwara, *Chem. – Eur. J.*, 2011, **17**, 7428; (*c*) J. D. Rinehart, M. Fang, W. J. Evans and J. R. Long, *Nat. Chem.*, 2011, **3**, 538; (*d*) J. D. Rinehart, M. Fang, W. J. Evans and J. R. Long, *J. Am. Chem. Soc.*, 2011, **133**, 14236; (*e*) R. J. Blagg, C. A. Muryn, E. J. L. McInnes, F. Tuna and R. E. P. Winpenny, *Angew. Chem., Int. Ed.*, 2011, **50**, 6530.
6 (*a*) C. R. Ganivet, B. Ballesteros, G. de la Torre, J. M. Clemente-Juan, E. Coronado and T. Torres, *Chem. – Eur. J.*, 2013, **19**, 1457; (*b*) S. K. Langley, D. P. Wielechowski, V. Vieru, N. F. Chilton, B. Moubaraki, L. F. Chibotaru and K. S. Murray, *Chem. Sci.*, 2014, **5**, 3246; (*c*) K. C. Mondal, A. Sundt, Y. Lan, G. E. Kostakis, O. Waldmann, L. Ungur, L. F. Chibotaru, C. E. Anson and A. K. Powell, *Angew. Chem., Int. Ed.*, 2012, **51**, 7550; (*d*) N. F. Chilton, *Inorg. Chem.*, 2015, **54**, 2097.
7 (*a*) N. Ishikawa, M. Sugita, T. Ishikawa, S. y. Koshihara and Y. Kaizu, *J. Am. Chem. Soc.*, 2003, **125**, 8694; (*b*) R. J. Blagg, L. Ungur, F. Tuna, J. Speak, P. Comar, D. Collison, W. Wernsdorfer, E. J. L. McInnes, L. F. Chibotaru and R. E. P. Winpenny, *Nat. Chem.*, 2013, **5**, 673; (*c*) N. F. Chilton, C. A. P. Goodwin, D. P. Mills and R. E. P. Winpenny, *Chem. Commun.*, 2015, **51**, 101.
8 T. Gupta, T. Rajeshkumar and G. Rajaraman, *Phys. Chem. Chem. Phys.*, 2014, **16**, 14568.
9 C.-H. Chen, K. B. Ghiassi, M. R. Cerón, M. A. Guerrero-Ayala, L. Echegoyen, M. M. Olmstead and A. L. Balch, *J. Am. Chem. Soc.*, 2015, **137**, 10116.
10 (*a*) R. Westerström, J. Dreiser, C. Piamonteze, M. Muntwiler, S. Weyeneth, H. Brune, S. Rusponi, F. Nolting, A. Popov, S. Yang, L. Dunsch and T. Greber, *J. Am. Chem. Soc.*, 2012, **134**, 9840; (*b*) R. Westerström, J. Dreiser, C. Piamonteze, M. Muntwiler, S. Weyeneth, K. Krämer, S.-X. Liu, S. Decurtins, A. Popov, S. Yang, L. Dunsch and T. Greber, *Phys. Rev. B: Condens. Matter Mater. Phys.*, 2014, **89**, 060406.
11 (*a*) L. J. Wilson, D. W. Cagle, T. P. Thrash, S. J. Kennel, S. Mirzadeh, J. Michael Alford and G. J. Ehrhardt, *Coord. Chem. Rev.*, 1999, **190–192**, 199; (*b*) T. Zuo, L. Xu, C. M. Beavers, M. M. Olmstead, W. Fu, T. D. Crawford, A. L. Balch and H. C. Dorn, *J. Am. Chem. Soc.*, 2008, **130**, 12992.
12 W. Fu, J. Zhang, T. Fuhrer, H. Champion, K. Furukawa, T. Kato, J. E. Mahaney, B. G. Burke, K. A. Williams, K. Walker, C. Dixon, J. Ge, C. Shu, K. Harich and H. C. Dorn, *J. Am. Chem. Soc.*, 2011, **133**, 9741.
13 (*a*) L. F. Chibotaru and L. Ungur, *J. Chem. Phys.*, 2012, **137**, 064112; (*b*) F. Aquilante, L. De Vico, N. Ferré, G. Ghigo, P.-å. Malmqvist, P. Neogrády, T. B. Pedersen, M. Pitoňák, M. Reiher, B. O. Roos, L. Serrano-Andrés, M. Urban, V. Veryazov and R. Lindh, *J. Comput. Chem.*, 2010, **31**, 224.
14 S. K. Singh, N. K. Tibrewal and G. Rajaraman, *Dalton Trans.*, 2011, **40**, 10897.
15 K. Furukawa, S. Okubo, H. Kato, H. Shinohara and T. Kato, *J. Phys. Chem. A*, 2003, **107**, 10933.
16 X. Dai, Y. Gao, M. Xin, Z. Wang and R. Zhou, *J. Chem. Phys.*, 2014, **141**, 244306.
17 T. Rajeshkumar and G. Rajaraman, *Chem. Commun.*, 2012, **48**, 7856.
18 A. Weber, O. Schiemann, B. Bode and T. F. Prisner, *J. Magn. Reson.*, 2002, **157**, 277.
19 S. K. Singh and G. Rajaraman, *Dalton Trans.*, 2013, **42**, 3623.
20 (*a*) L. Ungur, M. Thewissen, J.-P. Costes, W. Wernsdorfer and L. F. Chibotaru, *Inorg. Chem.*, 2013, **52**, 6328; (*b*) L. Ungur and L. F. Chibotaru, *Phys. Chem. Chem. Phys.*, 2011, **13**, 20086.